Eur. Phys. J. D **5**, 447–452 (1999)

THE EUROPEAN PHYSICAL JOURNAL D
EDP Sciences

Effects of a modulation of the pump-polarization in a degenerate pump/probe experiment

H. Mesnil, M.C. Schanne-Klein, and F. Hache[a]

Laboratoire d'Optique Quantique du CNRS, École Polytechnique, 91128 Palaiseau Cedex, France

Received: 21 July 1998 / Revised: 28 October 1998 / Accepted: 20 November 1998

Abstract. The effects of the pump-polarization in a degenerate pump/probe experiment are analyzed. It is shown that modulating the pump polarization from linear to circular induces a modulation in the probe absorption change that allows to separate various contributions that are mixed in the signal. An experimental demonstration is carried out in a laser dye (Coumarin 500).

PACS. 42.50.Md Optical transient phenomena: quantum beats, photon echo, free-induction decay, dephasings and revivals, optical nutation, and self-induced transparency – 42.81.Gs Birefringence, polarization

1 Introduction

Pump-probe experiments have been used for more than two decades to study the dynamics of many materials [1]. In these experiments, a first intense laser pulse is absorbed by the sample, leading to an excitation of its constituents. This excitation is then probed by a second, weak pulse, delayed with respect to the pump. This technique is very powerful and has been used in many time regimes (microsecond to femtosecond) and with a lot of various solid and liquid materials. The simplest form of the experiment is a one-laser (degenerate) technique, where a unique laser pulse is splitted into two parts, one for the excitation beam and the other for the probe one. Despite its simplicity, measurement of the transmission of the probe *versus* the delay between the two beams allows to determine significant lifetimes in the materials [2,3]. This technique has been considerably improved by using femtosecond tunable lasers that allow to have different wavelengths for the pump and the probe beams, giving rise to many sophisticated experiments, such as ultrafast photochemistry or wavepacket motion studies [4].

In the degenerate technique, a complication arises when the delay between the pump and the probe beams is close to zero, *i.e.* when the two beams overlap temporally in the sample. In that case, on top of the expected change of transmission following the excitation of the molecules, there is another signal coming from the coherent coupling between both beams (coherent artifact). This subtle effect has been studied in the 80's for pump-probe experiments [5–7] as well as optical Kerr shutter [8] and optical phase conjugation [6,9]. More sophisticated exploitation of the coherent coupling, based on a phase-sensitive interferometric detection have been proposed [10] and utilized to measure nonlinear susceptibilities and time response with a femtosecond resolution. All these experiments have been performed with linearly polarized beams. In this paper, we present a further development of this technique as well as of the study of the coherent coupling by examining the effect of circularly-polarized light. In particular, we show theoretically and experimentally that utilizing a polarization-modulated pump gives rise to new interesting features that can bring information on the coherence of the light beams as well as on the relevant relaxation times of the sample.

In a theoretical section (Sect. 2), we first derive the change of transmission, including the coherent artifact, for various polarizations of the pump and the probe beams and analyze the consequence of the pump polarization modulation. Then we present an experimental evidence of this effect in Section 3 on a laser dye (Coumarin 500). In Section 4, we discuss our experimental results and show that with our measurements we can separate two different phenomena taking place in the excited molecules (bleaching and induced absorption), a non-expected feature for this kind of measurement.

2 Theory

Calculation of the change of transmission of a weak probe beam due to a strong pump pulse has been studied a lot in the 80's, when the experimental techniques have been developed [11]. It has been known since then that, when one uses a unique wavelength for the two beams, one must be careful when calculating this change and take properly

---

[a] e-mail: `hache@leonardo.polytechnique.fr`

into account the coherent coupling between the beams (coherent artifact) [5–7]. In this section, we want to extend these calculations to the case of various polarization combinations, and in particular to the case of circularly-polarized beams.

In a pump-probe experiment, an excitation beam $E_e(t)$ is sent on the sample together with a delayed probe beam $E_p(t-\tau)$, where τ is the variable delay between the two beams. There is usually a small angle between these two beams, but taking this angle into account doesn't change qualitatively the following discussion and makes the expressions more complicated. We will therefore neglect it and suppose that the beams are plane waves which propagate along the z direction and are polarized in the x–y plane.

Following references [5–7], we introduce a response function $A(t)$. The change in the transmitted energy of the probe is made up of two terms:

$$\Delta E_p(\tau) \propto \gamma(\tau) + \beta(\tau) \tag{1}$$

where

$$\gamma(\tau) = \int_{-\infty}^{+\infty} dt \int_{-\infty}^{+\infty} dt' E^*_{p_i}(t-\tau) E_{p_j}(t-\tau) \times E_{e_k}(t') E_{e_l}(t') A_{ijkl}(t-t') \tag{2}$$

is the noncoherent contribution and

$$\beta(\tau) = \int_{-\infty}^{+\infty} dt \int_{-\infty}^{+\infty} dt' E^*_{p_i}(t-\tau) E_{e_j}(t) \times E^*_{e_k}(t') E_{p_l}(t'-\tau) A_{ijkl}(t-t') \tag{3}$$

is the coherent artifact. In these formula, i, j, k, l stand for the three space coordinates x, y, z and a summation over them is supposed. The difference between γ and β is clear: in γ, the probe beam is calculated only at $t-\tau$ and the pump one only at t', so that there is no need to have overlap of the beams ($t-t'$ may be longer than the pulse duration), and γ only involves the intensities of the beams. On the opposite, in β, the probe (pump) beam is calculated at $t-\tau$ and $t'-\tau$ (t and t') and will vanish as soon as the two beams no longer overlap. β involves the electric field amplitude and is phase-dependent and, as a consequence, will be non zero only if $t-t'$ is shorter than the coherence length of the pulses. Note that when the pulses are not transform-limited, another coherent coupling due to a phase grating can contribute [12], but it will prove to be irrelevant in our case.

Before discussing the origin and the symmetry of the response function, we want to derive the expression of γ and β for the various polarization combinations. Let us write the electric fields as

$\mathbf{E}_e = E(t)e^{i(kz-\omega t)}\widehat{\mathbf{e}}_e$ for the excitation beam and $\mathbf{E}_p = \varepsilon E(t)e^{i(kz-\omega t)}\widehat{\mathbf{e}}_p$ for the probe where $E(t)$ is the complex amplitude, k and ω the wavevector and the angular frequency of the light and $\widehat{\mathbf{e}}_{e,p}$ the polarization vectors and where $\varepsilon \ll 1$ is the ratio between the probe and pump amplitudes. Then we can express γ and β as:

$$\gamma(\tau) = \varepsilon^2 \int_{-\infty}^{+\infty} dt \int_{-\infty}^{+\infty} dt' \left|E(t-\tau)\right|^2 \times \left|E(t')\right|^2 F_\gamma(t-t') \tag{4}$$

$$\beta(\tau) = \varepsilon^2 \int_{-\infty}^{+\infty} dt \int_{-\infty}^{+\infty} dt' \times E^*(t-\tau)E(t)E^*(t')E(t'-\tau)F_\beta(t-t'). \tag{5}$$

It is possible to express F_γ and F_β as a combination of the independent components of the response function relevant for an isotropic medium: A_{xxyy}, A_{xyyx}, A_{xyxy}. The parallel component A_{xxxx} is connected to these components by $A_{xxxx} = A_{xxyy} + A_{xyyx} + A_{xyxy}$ [13].

For a linearly-polarized light, the polarization vectors are $\widehat{x}$ (noted $\|$) or $\widehat{y}$ ($\perp$) whereas for a circularly-polarized light, they are $(1/\sqrt{2})(\widehat{x} \pm i\widehat{y})$($C\pm$), $C+$ (resp. $C-$) corresponding to a left (resp. right)-handed polarization. It is possible to calculate F_γ and F_β for the different polarization combinations. The results are summarized in Table 1.

Let us now discuss the origin and symmetry of the response function. After absorption of light from the excitation beam by a molecule, the molecule reaches an excited state (usually a combination of electronic and vibrational excited states) and consequently, the absorption decreases (bleaching). As long as the configuration of the electronic levels involved in the optical transitions is fixed, this process can be seen as a $\chi^{(3)}$ process, and the symmetry of this nonlinear susceptibility tensor applies to the symmetry of the function response. In a liquid, one has to average over the molecular orientations to get the resultant isotropic tensor and we have:

$$\chi^{(3)}_{xxyy} = \chi^{(3)}_{xyyx} = \chi^{(3)}_{xyxy} = \frac{1}{3}\chi^{(3)}_{xxxx} \tag{6}$$

(x, y, z can be interchanged).

On the other hand, if there is a change of the level configuration subsequent to the the optical excitation, this $\chi^{(3)}$ picture does not apply any more. In that case, there is no direct relationship between the first transition (excitation stage) and the second one (probing stage). The process can therefore be seen as a cascade of two $\chi^{(1)}$ effects, and the symmetry of the response function is given by that of the $\chi^{(1)}\chi^{(1)}$ tensor. For a liquid with isotropic averaging, we have

$$\chi^{(1)}_{ij} = \chi^{(1)}_{xx}\delta_{ij} \tag{7}$$

and consequently

$$\begin{aligned} \chi^{(1)}_{xx}\chi^{(1)}_{xx} &= \chi^{(1)}_{xx}\chi^{(1)}_{yy} \neq 0, \\ \chi^{(1)}_{xy}\chi^{(1)}_{xy} &= \chi^{(1)}_{xy}\chi^{(1)}_{yx} = 0. \end{aligned} \tag{8}$$

As a general expression, we can write the response function, following reference [6]

$$A_{ijkl} = B\chi^{(1)}_{ij}\chi^{(1)}_{kl} + C\chi^{(3)}_{ijkl}, \tag{9}$$

Table 1. Expressions of F_γ and F_β in the general case and for a liquid. The pump and the probe polarizations can be indifferently polarization 1 or 2 ($\rho = A_{xxyy}/A_{xxxx}$).

Polarizations		General case		Liquid	
1	2	F_γ	F_β	F_γ	F_β
$\parallel$	$\parallel$	A_{xxxx}	A_{xxxx}	1	1
$\parallel$	$\perp$	A_{xxyy}	A_{xyyx}	ρ	$(1-\rho)/2$
$\parallel, \perp$	C_+, C_-	$\frac{1}{2}(A_{xxxx}+A_{xxyy})$	$\frac{1}{2}(A_{xxxx}+A_{xyyx})$	$(1+\rho)/2$	$(3-\rho)/4$
C_+	C_+	$\frac{1}{2}(A_{xxxx}+A_{xxyy}+A_{xyyx}-A_{xyxy})$	$\frac{1}{2}(A_{xxxx}+A_{xxyy}+A_{xyyx}-A_{xyxy})$	$(1+\rho)/2$	$(1+\rho)/2$
C_+	C_-	$\frac{1}{2}(A_{xxxx}+A_{xxyy}-A_{xyyx}+A_{xyxy})$	$\frac{1}{2}(A_{xxxx}-A_{xxyy}+A_{xyyx}+A_{xyxy})$	$(1+\rho)/2$	$1-\rho$

B taking into account the loss of memory of the initial configuration of the molecules. There may be many physical origins to this loss. The most obvious one is the orientational relaxation of the molecules [6]. The absorption of light will depend on the orientation of the molecules with respect to the direction of the electric field, and a change of orientation will affect the subsequent absorption. For times long compared to the orientational relaxation time, only the B term will be important. This process is however not relevant in our experiments, because it takes hundreds of picoseconds for large dye molecules to reorient in common solvents [14]. On our sub-ps timescale, the reorientation of molecules is therefore completely negligible. Other mechanisms can come into play. For example, if subsequently to an optical absorption, the shape of the molecule or the arrangement of the solvent molecules change, this can translate into a partial loss of the initial configuration. These changes can occur very rapidly, and one can therefore get a stationary response function with non zero B and C. Measurement of the ratio B/C gives an estimation of the memory of the initial configuration in the excited molecule.

Inserting equations (6, 8) in equation (9), we get

$$A_{xxxx} = B\chi^{(1)}_{xx}\chi^{(1)}_{xx} + C\chi^{(3)}_{xxxx} \tag{10a}$$

$$A_{xxyy} = B\chi^{(1)}_{xx}\chi^{(1)}_{xx} + \frac{1}{3}C\chi^{(3)}_{xxxx} \tag{10b}$$

$$A_{xyyx} = A_{xyxy} = \frac{1}{3}C\chi^{(3)}_{xxxx}. \tag{10c}$$

Note that the equality $A_{xyyx} = A_{xyxy}$ is not the usual equality expected for a $\chi^{(3)}$ tensor. With our definition, the relevant $\chi^{(3)}$ in the frequency space is $\chi^{(3)}(\omega, -\omega, \omega)$ and the equality that comes from the general permutation rules is $\chi^{(3)}_{xyyx} = \chi^{(3)}_{xxyy}$. This remark allows to understand better the calculation of reference [5] where a confusion is made between $\chi^{(3)}$ and A.

Following reference [5], we can introduce the "depolarization factor"

$$\rho = \frac{A_{xxyy}}{A_{xxxx}} \cdot \tag{11}$$

The value of ρ is comprised between 1/3 when $B = 0$ and 1 when $C = 0$. It is therefore another way to measure the loss of memory of the system. This parameter is connected to the ratio B/C by:

$$\frac{B\chi^{(1)}_{xx}\chi^{(1)}_{xx}}{C\chi^{(3)}_{xxxx}} = \frac{\rho - 1/3}{1-\rho} \cdot \tag{12}$$

With this parameter, we also have

$$\frac{A_{xyyx}}{A_{xxxx}} = \frac{A_{xyxy}}{A_{xxxx}} = \frac{1-\rho}{2} \cdot \tag{13}$$

Using ρ, we can rewrite the expression of F_γ and F_β for a liquid in relative units (see last columns in Tab. 1), and analyze the effect of a modulation of the polarization of the pump on the change of transmission of the probe. A remarkable point is that if the probe is circularly-polarized, the non-coherent part of the signal (F_γ) is constant, whereas it is not the case for the coherent artifact (F_β). In Figure 1, we have schematically drawn the results when the polarization of the pump is modulated in time: the abscissa represents the polarization of the pump and the ordinate is F_γ (incoherent signal) and $F_\gamma + F_\beta$, (total signal at zero delay). Figure 1a is for a linearly-polarized probe and Figure 1b for a circularly-polarized one ($C+$). If the probe is linearly-polarized, both contributions have the same behaviour and the signal exhibits a modulation at twice the frequency of the pump polarization modulation. On the other hand, if the probe is circularly-polarized, there is no modulation for the non-coherent part but the coherent artifact is modulated at the same frequency. This is a way to single out the coherent artifact and to measure the coherence of the laser pulses. We can extract more information from this modulated coherent artifact: looking at Table 1, one can see that the peak-to-peak modulation is connected to $A_{xxyy} - A_{xyxy} = B\chi^{(1)}_{xx}\chi^{(1)}_{xx}$ (see Eqs. (10)). That means that this signal is directly a measure of the loss of the initial configuration of the molecules. On the other hand, if one looks at the non-coherent part of the $2f$-modulated signal for a linear probe (Fig. 1a), one gets a signal equal to $A_{xxxx} - A_{xxyy} = -(2/3)C\chi^{(3)}_{xxxx}$. In that case, the B term does not contribute and only the $\chi^{(3)}_{xxxx}$ part of the signal is observed. Following the temporal evolution of this signal is a way to single out this contribution.

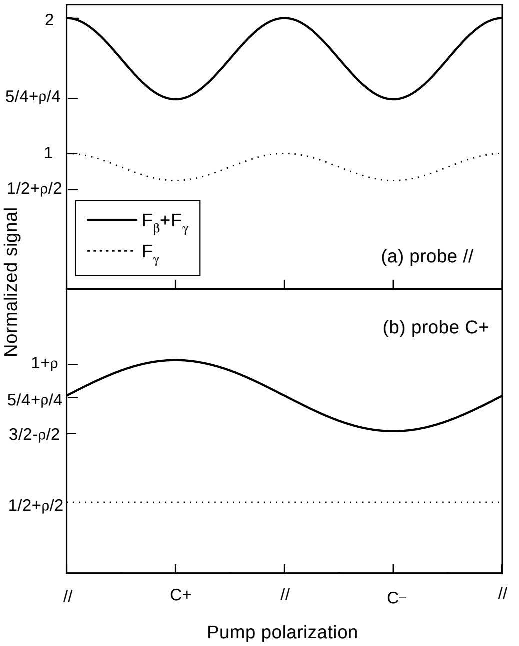

Fig. 1. Schematic of the non-coherent (F_γ) and total ($F_\beta + F_\gamma$) signal measured when the pump polarization is modulated for two probe polarizations: (a) $\|$, (b) C_+.

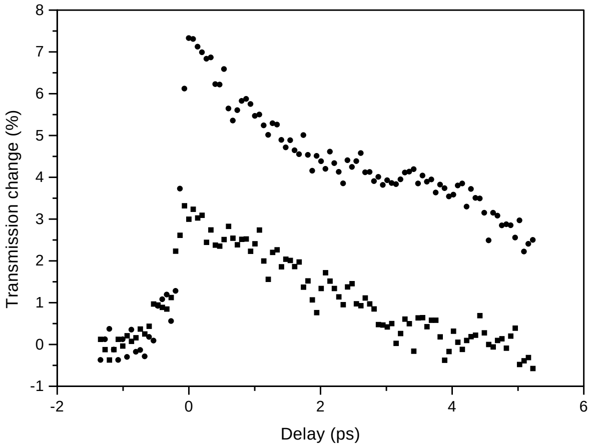

Fig. 2. Transmission change *vs.* pump/probe delay for two probe polarizations: $\|$ (dots) and $\perp$ (squares). The pump polarization is fixed ($\|$).

3 Experiment

To verify experimentally the results of the preceding section, we set-up a classical pump-probe experiment in a laser dye Coumarin 500. This dye has a sharp absorption peak centered at 395 nm and a strong luminescence centered at 499 nm when diluted in Ethanol. We use a concentration of 2.4×10^{-4} M, the optical density at 400 nm for the sample being ~ 1.3.

The excitation laser is a frequency-doubled Ti:sapphire laser, delivering fs pulses at 1 kHz. The frequency doubling is performed in a 2.5 mm-thick BBO crystal, leading to fairly long 400 nm-pulses (around 250 fs). We use these pulses without any compression. The pulse energy is less than 1 μJ, which is sufficient to give measurable effects without inducing undesirable thermal or higher-order effects. The pulses are splitted in two parts by a glass plate. The weakest part serves as the probe beam and the strongest one as the pump. Initial polarization of the beams is carefully controlled by film polarizers. The two beams are collimated through two $f = 250$ mm lenses on a circulating 3 mm-thick cell containing the laser dye, with an external angle of 2°. By use of compensated zero-order quartz half-and quarter-waveplates, we control the polarization of the probe. Four configurations are used: $\|$, $\perp$, $C\pm$. The pump beam is sent through a KDP Pockels cell on which we apply a sinusoidal voltage at a frequency $f = 88$ Hz. The peak voltage is ± 350 V, which corresponds to the quater-wave voltage for 400 nm. The pump polarization is therefore modulated and changes as $\| \to C_+ \to \| \to C_- \to \|$ at the frequency f. We have carefully checked that for the maximum voltage, our setup is equivalent to a $\lambda/4$ plate to better than 4%, indicating that we get a good circular polarization. All the optics (especially the focusing lenses) are also carefully aligned so as to preserve the state of polarization of both beams inside the sample. The probe beam is measured with a photomultiplier tube (PMT), the output of which is sent to a computer and to a lock-in amplifier. For each measurements we get the direct (PMT) signal and the lock-in signal together. These signals are then recorded *versus* the delay between the pump and the probe beams.

Figure 2 shows the change of transmission of the probe when the pump polarization is not modulated, but fixed as $\|$. $\|$ and $\perp$ probe polarizations are plotted. The two curves have very similar shapes, and the ratio between them is fairly constant ($\sim 2.6 \pm 0.1$) for positive delays between the two beams. This ratio corresponds to $\rho = 0.39 \pm 0.01$. The coherent artifact is not clearly seen in these curves, as it is indistinguishable from the rise of the signal [5].

We want now to check the implications of our calculations, and we modulate the pump polarization. In Figure 3 are plotted the lock-in signal at f and $2f$ for a $\|$-polarized probe and at $2f$ for a $\perp$-polarized one. The results are in perfect agreement with the previous section: as only a $2f$-modulation is expected in that case (see Fig. 1a), no signal is observed at f whereas non-zero signals are obtained at $2f$. We observe a change of sign between the $\|$ and $\perp$ curves, which is consistent with the previous results. Indeed, from Table 1, one can see that the peak-to-peak modulation in F_γ is $1 - (1 + \rho/2) = (1 - \rho)/2$ in the $\|$ case and $\rho - (1 + \rho/2) = -(1 - \rho)/2$ in the $\perp$ one. The ratio between the peak-to-peak modulated signal ($= (1-\rho)/2$) and the average PMT signal ($= (3+\rho)/4$) is measured to be 0.38 ± 0.01, from which we can calculate $\rho = 0.36 \pm 0.02$.

If we consider now a circularly-polarized probe beam, we get the curves plotted in Figure 4 for the lock-in signal at f. We only observe one sharp peak that changes signs when the probe polarization is changed from C_+ to C_-, in accordance with Figure 1. This peak is clearly the coherent artifact as expected from the calculation. The height

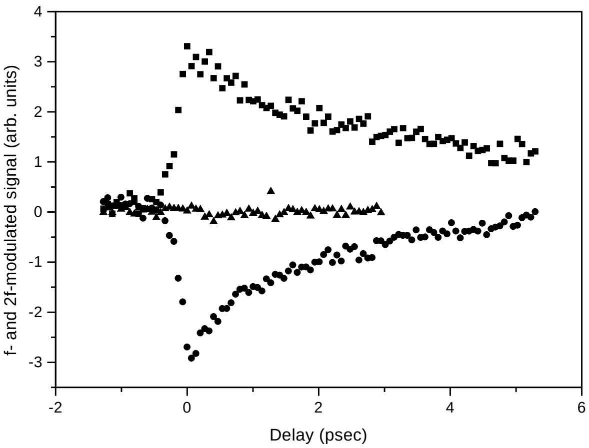

Fig. 3. f- and $2f$-modulated probe transmission change *vs.* pump/probe delay. Squares and dots: $2f$-signal for a $\parallel$ and $\perp$ polarized probe, triangles: f-signal.

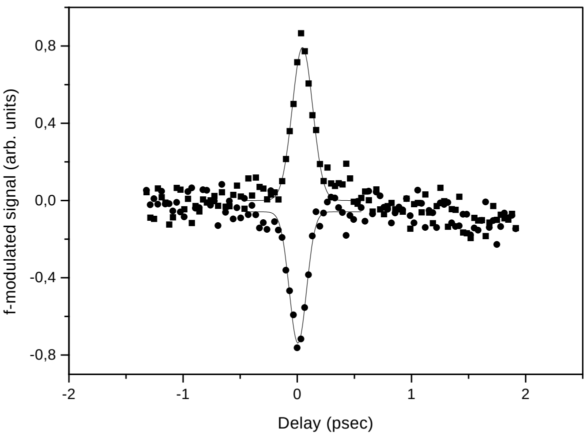

Fig. 4. f-modulated probe transmission change *vs.* pump/probe delay for a circularly-polarized probe. Squares: C_+, dots: C_-. The solid lines are Gaussian fits.

of this peak is $\sim 5 \pm 1\%$ of the PMT signal, from which we can get $\rho = 0.38 \pm 0.01$. Its width (FWHM) is about 240 fs, corresponding to a deconvoluted coherence time of the pulse equal to 170 fs. It is shorter than the pulse duration because the latter is artificially increased during the second-harmonic generation process due to the group-velocity mismatch between the fundamental and the harmonic pulses in the BBO crystal. Note however that the coherent peak is symmetrical, ruling out the contribution of a phase grating [12].

From the above experiments, we have been able to get three independent measurements of ρ; the consistency of these values clearly demonstrates the validity of the previous calculations.

4 Discussion

First of all, we observe that $\rho = 0.38$ is slightly different from 1/3, which implies that there is a partial loss of memory of the initial configuration and we calculate $B\chi^{(1)}_{xx}\chi^{(1)}_{xx}/C\chi^{(3)}_{xxxx} = 0.08$. An important conclusion can be drawn from Figure 2: one can remark that the $\parallel$ and $\perp$ curves are decreasing with the same time constant. This proves that the value of ρ does not change on this time scale. If ρ should change, the $\perp$ curve should not follow the $\parallel$ one but reflect the change in ρ. This means that the configuration change in the excited state is very rapid, in agreement with [3]. It is well-known that in coumarins, the excited state is much more polar than the fundamental one with the permanent dipole increasing by several Debyes [15] and that optical excitation is accompanied by a charge transfer [17]. We believe that this is the origin of the instantaneous loss of configuration that we measure. It is important to notice that examination of Figure 2 alone would not be sufficient to ascertain that $B \neq 0$, especially for short time delays; however, the existence of a non-zero f-modulated signal for a circularly-polarized probe (Fig. 4) gives a definite evidence of this, since this signal is only sensitive to B.

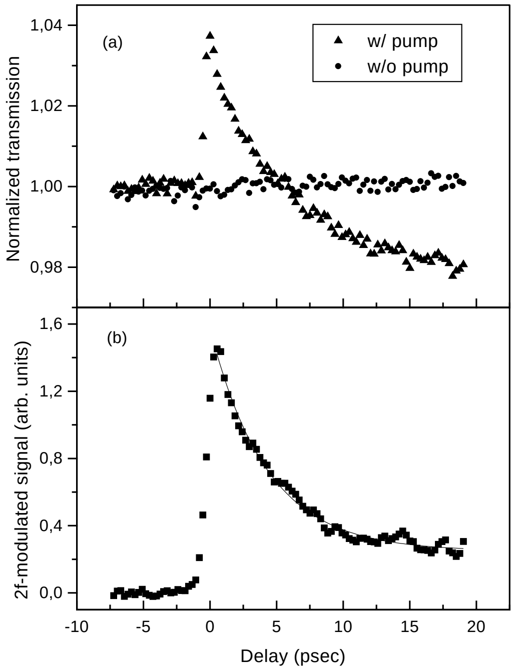

Fig. 5. (a) Normalized transmission of a $\parallel$ polarized probe *vs.* pump/probe delay with and without the pump. (b) $2f$-modulated signal when the pump is present. The solid line is an exponential fit ($\tau = 4$ ps).

As already stated, we expect the $2f$-modulated signal to reflect the $\chi^{(3)}$ behaviour of the molecules whereas the total signal may be a combination of various contributions. A demonstration of this is given in Figure 5 where we have plotted the PMT (Fig. 5a) and the $2f$-modulated signal (Fig. 5b) on a longer (20 ps) timescale. We observe that the two curves are different. The $2f$-curve displays a simple behaviour with a (non resolved) rise and an exponential decay ($\tau = 4$ ps) to a non-zero value. On the other hand, the PMT signal is more complicated and one clearly sees that there is a change of sign of the signal. Considering the energies involved, thermal effects can be discarded

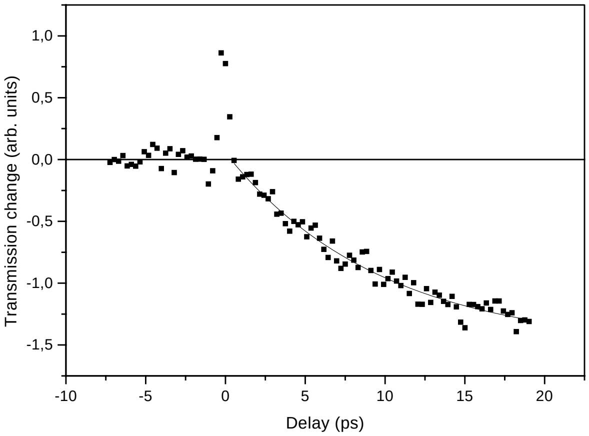

Fig. 6. Excited-state absorption *vs.* pump/probe delay as deduced from Figure 5 (see text). The solid line is an exponential fit ($\tau = 10$ ps).

(especially in a laser dye where most of the de-excitation occurs *via* fluorescence), but we can propose a straightforward interpretation of this last result. In coumarin, the excitation at the maximum of absorption is from the bottom of the S_0-state to a vibrationally excited S_1-state. After the optical excitation, there is an internal vibrational relaxation toward the bottom of the S_1-state, responsible for the decrease of the observed bleaching. When the molecules are in this state, they mostly get de-excited by emission of fluorescence (and for a very small fraction, by transition to the triplet state and subsequent phosphorescence). Fluorescence lifetimes are in the nanosecond range and we don't expect a full recovery of the absorption on a picosecond timescale. This is indeed what we observe in the $2f$-signal, which describes only the bleaching process. To explain the PMT signal, one must introduce some excited state absorption $S_1 \to S_n$. Such absorption has already been observed in coumarins [16]. It means that on top of the bleaching, there is appearance of a new absorption signal, resulting in a change of sign of the PMT signal. Subtracting the two curves after adjustment of the peaks allows to extract from the PMT signal the excited state absorption, plotted in Figure 6. The peak at zero delay is due to the coherent artifact because the normalization procedure is not the same for F_β and F_γ. The signal for positive delays describes the building-up the excited-state absorption. We measure a rise time of 10 ps. This time is larger than the decay time of the $2f$-curve. We think that the reason for this is that the bleaching will decrease as soon as the molecules leave the excited S_1 state where they were promoted by the laser excitation, whereas the increase of induced absorption corresponds to the molecules reaching the bottom of the S_1 state. This second time is expected to be longer than the first one.

5 Conclusion

In this paper, we have analyzed the effect of a modulation of the polarization of the pump (from linear to circular) in a degenerate pump/probe experiment. In particular, the resulting modulation of the non-coherent signal as well as the coherent artifact have been carefully examined and we have shown that looking at the probe absorption change modulated at the frequency of the pump polarization modulation or at its second harmonic allows to separate various contributions that are mixed in the signal: coherent artifact, bleaching, induced absorption. An experimental demonstration has been carried out with a laser dye, Coumarin 500 and two relevant times (decay time of the bleaching, rise time of the induced absorption) have been determined. The separation between bleaching and induced absorption clearly demonstrates the potentiality of this technique. These results show that the well-known degenerate pump-probe technique, although very simple, is very powerful and that a straightforward extension allows to get easily very interesting results, not expected at first glance, without requiring sophisticated setups. In particular, studying the coherent artifact brings information on the loss of memory that occurs at short times in the molecules after an optical excitation. This technique could be used with shorter pulses to resolve experimentally such effects that are connected to molecular rearrangements or solvent redistribution.

We thank G.M. Gale for a careful reading of the manuscript.

References

1. See for example, *Ultrafast Phenomena IV*, edited by D.H. Auston, K.B. Eisenthal (Springer, Berlin, 1984).
2. E.P. Ippen, C.V. Shank, A. Bergman, Chem. Phys. Lett. **38**, 611 (1976).
3. T. Joo, Y. Jia, J.Y. Yu, M.J. Lang, G.R. Fleming, J. Chem. Phys. **104**, 6089 (1996).
4. See for example, *Ultrafast Phenomena X*, edited by P.F. Barbara, J.G. Fujimoto, W.H. Knox, W. Zinth (Springer, Berlin, 1996).
5. Z. Vardeny, J. Tauc, Opt. Commun. **39**, 396 (1981).
6. B.S. Wherrett, A.L. Smirl, T.F. Boggess, IEEE J. Quant. Electron. **QE19**, 680 (1983).
7. T.F. Heinz, S.L. Palfrey, K.B. Eisenthal, Opt. Lett. **9**, 359 (1984).
8. J.L. Oudar, IEEE J. Quant. Electron. **QE19**, 713 (1983).
9. F. Hache, P. Rousignol, D. Ricard, C. Flytzanis, Opt. Commun. **64**, 200 (1987).
10. L. Sarger, P. Segonds, L. Canioni, F. Adamietz, A. Ducasse, E. Fargin, C. Duchesne, R. Olazcuaga, G. Le Flem, J. Opt. Soc. Am. B **11**, 995 (1994).
11. R.W. Hellwarth, Prog. Quant. Electr. **5**, 1 (1977).
12. S.L. Palfrey, T.F. Heinz, J. Opt. Soc. Am. B **4**, 674 (1985).
13. See for example, P.N. Butcher, D. Cotter, *The Elements of Nonlinear Optics*, edited by P.L. Knight, W.J. Firth (Cambridge University Press, 1990), p. 142.
14. C.V. Shank, E.P. Ippen, Appl. Phys. Lett. **26**, 62 (1975).
15. P.K. McCarthy, G.J. Blanchard, J. Phys. Chem. **97**, 12205 (1993).
16. S.A. Kovalenko, J. Ruthmann, N.P. Ernsting, Chem. Phys. Lett. **271**, 40 (1997).
17. *Dye Lasers*, edited by F.P. Schäfer (Springer, Berlin, 1973), p. 161.